Nonlinear laser focusing using a conical guide and generation of energetic ions

Lihua Cao,[1] Wei Yu,[2,3] M. Y. Yu,[3,4] Han Xu,[5] X. T. He,[1,3,6] Yuqiu Gu,[7] Zhanjun Liu,[1] Jinghong Li,[1] and Chunyang Zheng[1]
[1]*Institute of Applied Physics and Computational Mathematics, P.O. Box 8009, Beijing 100088, China*
[2]*Shanghai Institute of Optics and Fine Mechanics, Chinese Academy of Sciences, Shanghai 201800, China*
[3]*Institute for Fusion Theory and Simulation, Department of Physics, Zhejiang University, Hangzhou 310027, China*
[4]*Institut für Theoretische Physik I, Ruhr-Universität Bochum, D-44780 Bochum, Germany*
[5]*National University of Defense Technology, Institute of Computer Science, Changsha 410073, China*
[6]*Center for Applied Physics and Technology, Peking University, Beijing 100871, China*
[7]*Laser Fusion Research Center, China Academy of Engineering Physics, Mianyang 621900, China*
(Received 2 January 2008; revised manuscript received 29 June 2008; published 17 September 2008)

Using conventional methods, a laser pulse can be focused down to around 6–8 μm, but further reduction of the spot size has proven to be difficult. Here it is shown by particle-in-cell simulation that with a hollow cone an intense laser pulse can be reduced to a tiny, highly localized, spot of around 1 μm radius, accompanied by much enhanced light intensity. The pulse shaping and focusing effect is due to a nonlinear laser-plasma interaction on the inner surface of the cone. When a thin foil is attached to the tip of the cone, the cone-focused light pulse compresses and accelerates the ions in its path and can punch through the thin target, creating highly localized energetic ion bunches of high density.

DOI: 10.1103/PhysRevE.78.036405 PACS number(s): 52.59.−f

I. INTRODUCTION

In strong-field sciences such as laser acceleration of charged particles to high energies, a key issue is to concentrate light energy into an extremely small time-space interval. The availability of femtosecond lasers opens a new era in this area. The interaction of an intense fs laser pulse with plasma can be significantly different from that of pico- and nanosecond laser pulses, and can lead to many interesting new effects and applications [1–3]. With the recent advances in ultrashort ultraintense (USUI) laser pulses with low emittance, generation of energetic ion bunches from the interaction of such lasers with foil targets has become realizable [1–10]. Such energetic ions can be important in proton therapy [11], fast ignition (FI) [4], and other modern applications. Depending on the target density and laser intensity [8], ions can be accelerated by several different mechanisms, such as very thin layers of target normal sheath acceleration (TNSA) at the target front and rear surfaces [12], shock acceleration inside the target [13,14], laser-piston acceleration of a small part of the target [15,16], direct laser acceleration of a small target [17], etc., as well as their combinations. In almost all of these mechanisms, the ions are mainly accelerated by the space-charge field created from the ejection of electrons in the target plasma by light pressure. The laser-piston acceleration mechanism [15] is apparently the most efficient. Particle-in-cell (PIC) simulations show that a target region of the size of the laser spot is pushed forward by the laser and accelerated as a whole. The ions therein can gain much energy, as in the direct acceleration of a small target [17]. But the scheme requires laser intensities two orders magnitude higher than that of the present-day lasers.

In practice, a laser pulse can be focused to 6–8 μm [18,19] with conventional methods. But it is difficult to focus an intense laser pulse to a spot of 1 μm or less. In this paper, we propose to "focus" (more accurately, to squeeze and reshape) a laser pulse by a hollow cone comparable in size with it. It is shown by PIC simulation that as a result of the nonlinear interaction with the inner cone surface, an intense laser pulse can be focused to a tiny spot of $\sim$1 μm radius, together with enhanced light intensity. Acting like an oblique target, the cone electrons interact with the (outer part of the) laser pulse as well as reconfigure the pulse structure. As a result, a highly concentrated thin light pulse is formed, accompanied by a loss of laser energy to the plasma and to reflection. We also show that if a thin foil target is placed across the focal spot at the open tip of the cone, the tiny cone-modified light pulse can efficiently punch through the foil plasma, accelerating and pushing out the target ions in front of it. Highly localized and energetic ion bunches of high density are produced. The result can be attributed to the highly localized laser pulse after the nonlinear cone focusing as well as the thin target. The ion bunch, but much smaller in cross section, resembles that from the laser-piston acceleration mechanism operating in a much higher laser-intensity ($a\sim 300$) and plasma-density ($n\sim 50n_c$) regime [15,16].

II. LASER FOCUSING BY CONICAL TARGET

A tiny hollow metal cone was first introduced in recent FI experiments to shield the igniting laser pulse from the underdense region of the precompressed fuel plasma [20,21]. A remarkable increase in the thermal fusion-neutron yield was observed. PIC simulations showed that a cone-shaped target can nonlinearly guide and focus a laser beam [22,23]. In their simulations the laser used is a semi-infinite beam and the cone tip is closed, so that the laser interacts strongly with the cone. Both two-dimensional (2D) and three-dimensional simulations were performed and the conclusions were similar [22].

In this paper, instead of a semi-infinite beam (standing wave), we consider a short Gaussian pulse, and instead of a hollow cone closed at the tip, we consider a cone-shaped channel that is open at both ends, as shown in Fig. 1. Be-

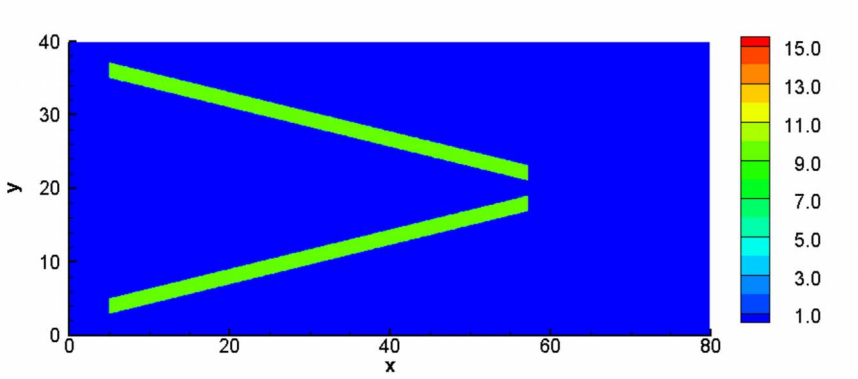

FIG. 1. (Color online) The open hollow-cone target for laser focusing. The diameters at the left and right openings are 30λ and 2λ, respectively. The cone angle is 30°, the target density is $10n_c$, and the laser pulse is launched from the left and converges at the front of the open hollow-cone target.

cause of the laser-plasma interaction at the cone wall, the pulse is nonlinearly guided and focused by the cone-shaped channel. For the simulation we use a 2D3V PIC code [24], which does not take into consideration encounters of the particles within the Debye sphere. An circularly polarized laser pulse with wavelength $\lambda=1.06$ μm has a Gaussian envelope $a=a_0\exp[-(t-t_0)^2/\tau^2]\exp[-(y-y_0)^2/w^2]$ in both the longitudinal (x) and transverse (y) directions. We shall set $a_0=4$, corresponding to a peak laser intensity of 4×10^{19} W cm^{-2}, $\tau=t_0=25T$, and $w=10\lambda$, and y_0 is in the middle line of the y axis, where $T=3.5$ fs is the laser period. The laser pulse incidents from the left along the x axis into the 30° cone shaped channel, as shown in Fig. 1. The diameters of the left and right cone openings are 30λ and 2λ, respectively. For simplicity, the cone is represented by a thin $(d=2\lambda)$ dense $(n=10n_c$, where n_c is the critical density) conical plasma. The 2D simulation box is 80λ long and 40λ wide. We apply the Lindmann condition [25] for the left boundary, periodic conditions for the top and bottom boundaries, and absorbing conditions for the right boundary. For the simulations, we use a spatial mesh (x,y) of 1024×512 cells and 25.6×10^6 each of electrons and protons, and the time step of the simulation is $0.05T$. The initial velocity distributions of the plasma electrons and ions are Maxwellian, with temperatures 4 and 1 keV, respectively. In the following presentations and figures, the spatial and time coordinates are normalized by λ and T, respectively, and the electron n_e and ion n_i densities by n_c. The momentum is normalized by mc, where m is the electron mass and c is the speed of light in vacuum. The electromagnetic (EM) energy density is $W=E^2+B^2$, where the electric (E) and magnetic and (B) fields are normalized by $m\omega_0c/e$, with e the electron charge and ω_0 the laser-light frequency.

Figure 2(a) shows the spatial distribution of the EM energy density at $t=89.51T$. After the laser pulse of initial spot radius 10λ enters the large left cone opening, it interacts with the electrons at the cone wall and is guided and reshaped until it reaches the small right opening. It then leaves the latter as a thin light pulse with a ~1 μm spot radius and 30° convergence angle. It keeps propagating forward for a distance of about a Rayleigh length, with the tiny spot radius remaining almost unchanged, before the latter gradually increases because of diffraction. Figure 2(b) shows the distribution of the electron density at $t=89.51T$. The cone electrons are compressed (and heated) by the laser light, which is in turn modulated by the self-consistently modified electron distribution in the cone plasma. This scenario differs from the standing-wave case of Silva *et al.* [14], Sentoku *et al.* [22], and Nakamura *et al.* [23] where a p-polarized laser is semitrapped at the closed-cone front and there is strong and prolonged interaction between the light and the cone plasma. In that case a considerable fraction of the laser energy is reflected and absorbed by the plasma, and hot electrons are produced. In contrast, here the hollow cone with both sides open acts as a lenslike guide that focuses or squeezes a pulse of spot radius 10λ into a tiny spot of radius $\sim1\lambda$, thereby greatly increasing its intensity. The radial compression or squeezing of the laser light by the hollow cone can be clearly seen in Fig. 3, showing the radial distribution of the EM energy density when the peak of the light pulse is at the left (black curve) and right (red curve) cone openings. In spite of laser light reflection and absorption by the cone wall due to the laser-plasma interaction, the tiny spot size [full width at half maximum (FWHM) $\sim0.5\lambda$] of the highly localized and

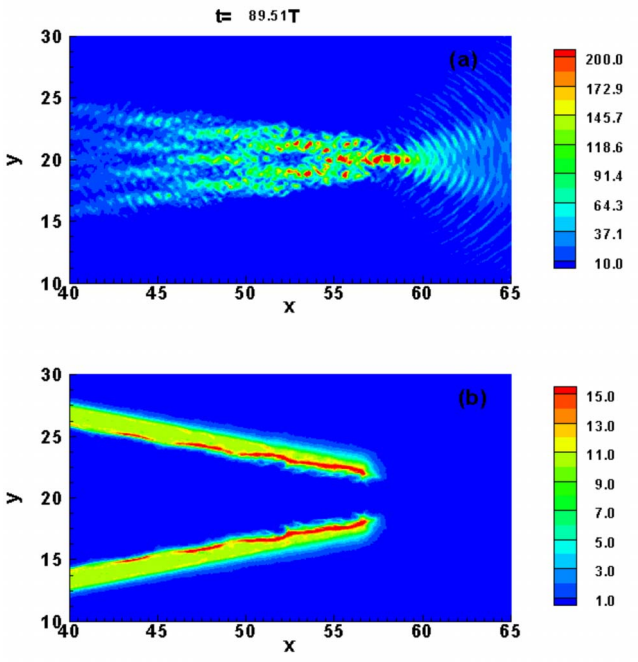

FIG. 2. (Color online) Distributions of the electromagnetic energy density (a), normalized by $(m\omega_0c/e)^2$, and the electron density (b), normalized by n_c, at $t=89.51T$.

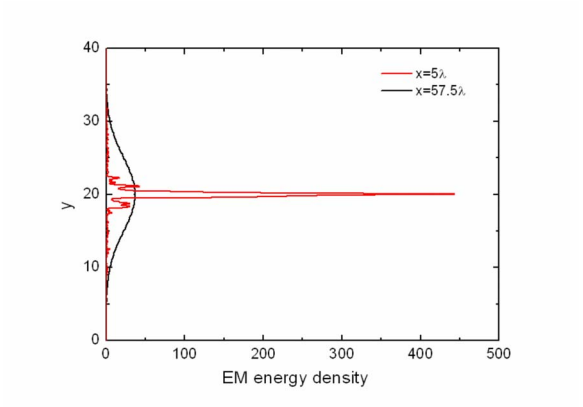

FIG. 3. (Color online) The radial distribution of electromagnetic energy density as the peak of laser pulse passes the left (black curve) and right (red curve) openings of the open hollow-cone target. Note that the exiting light pulse is of very small spot size.

intense light pulse at the right cone opening is just 10% of the input laser pulse and the peak intensity is also increased more than 10 times. In fact, about 10% and 47% of the incident laser energy flux is reflected and absorbed, respectively, by the cone electrons that are compressed and heated. The remaining 43% of the original energy is in the squeezed and focused (now much thinner) light pulse exiting the right opening of the cone channel.

III. GENERATION OF ENERGETIC ION BUNCHES

It is well known [8,10,16,26,27] that the mechanism and efficiency of ion acceleration in laser-target interaction depends on the thickness and density of the target, as well as the laser intensity. In particular, when the target is thin and not too dense, *all* the target ions facing the center of the laser pulse are set into motion. It follows that if the intensity of a light pulse is highly localized, as in the cone-focused light pulse here, an energetic ion bunch of very small cross section can be created. For investigating this possibility we attach a thin flat foil of thickness 1λ and density $10n_c$ to the tip of the cone [22,23] as shown in Fig. 4. The primary, or focusing, hollow-cone target remains the same as in Fig. 1. In the following discussion we shall mainly concentrate on the ion time scale, since the electron dynamics—namely, the ponderomotive evacuation of electrons and creation of a space-charge field—in the regime of interest is well known [1–3,29].

Figure 5 shows the distribution of the EM energy density (left column) and the ion density (right column) at $t=69.62T$, $82.05T$, and $89.51T$, respectively. Figures 5(a) and 5(b) show that at $t=69.62T$ the intense light pulse has strongly indented and pushed into the target, compressing the local ions and launching an electrostatic shock which accelerates the ions forward [13,14,30]. The maximum ion density is around $20n_c$, so that short-range collisions can still be ignored in the simulation. A very thin layer of TNSA ions can also be seen outside the back target surface [8,12]. Figures 5(c) and 5(d) show that at $t=82.05T$ the light pulse has displaced the target ions by pushing and compressing the target ions in front of it. We can see that all the ions facing the light pulse have been displaced forward. We note that at this stage the plasma is still not transparent to the laser. As expected [8], two groups of energetic ions appear in the ion density distribution. The leading group, of low density and wide spatial spread, is due to TNSA. The main group, in the form of a thin high-density layer, is due to shock acceleration, with the fastest ions at twice the shock speed. Figures 5(e) and 5(f) at $t=89.51T$ show that the center part of the foil has been almost completely punched out by the light pulse which is strongest on the propagation axis. The profile of the ion bunch thus becomes curved, with the highest-energy ions on the axis. The leading front of the plasma layer also becomes very thin (0.2λ), and its density is reduced to $\sim 3n_c$. This part of the target is then transparent, as can be clearly seen in Fig. 5(e). The very narrow distributions of the ion number and energy can be attributed to the correspondingly small space and time profiles of the cone-focused light pulse of tiny spot size. Figures 5(e) and 5(f) also show that despite the expected onset of diffraction, the light pulse is still tightly focused.

Figure 6 shows the ion energy density $(\gamma-1)n_i$ at $t=82.05T$, $84.53T$, and $89.51T$. Here, ions of lower energies have been omitted, so that the evolution of the most energetic ions can be more clearly observed. Note that the ions are almost monoenergetic. Tens-of-MeV ions have also been observed in existing simulations and experiments involving thin foils and other mechanisms [10,26–28]. However, here the spatial localization (FWHM $\ll 1\lambda$ in both the longitudinal and transverse directions) is much smaller than that from the existing ion acceleration schemes. Because of the much smaller bunch size, the number ($\sim 10^9$) of high-energy (tens

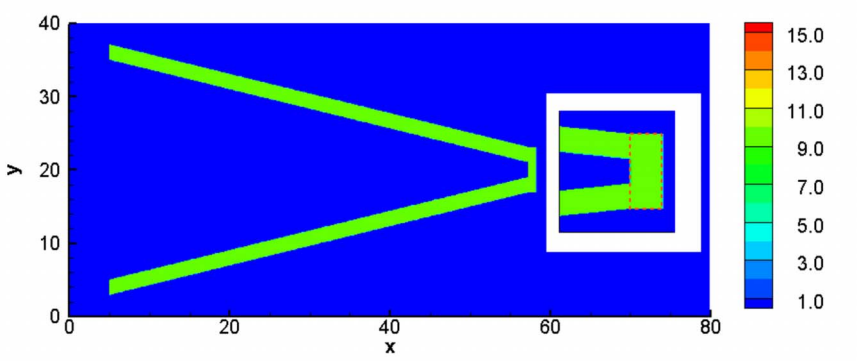

FIG. 4. (Color online) The cone-foil target for ion acceleration. The inset shows a foil (indicated by the red rectangle) with density $10n_c$ and thickness 1λ attached to the tip of the open hollow-cone target of Fig. 1.

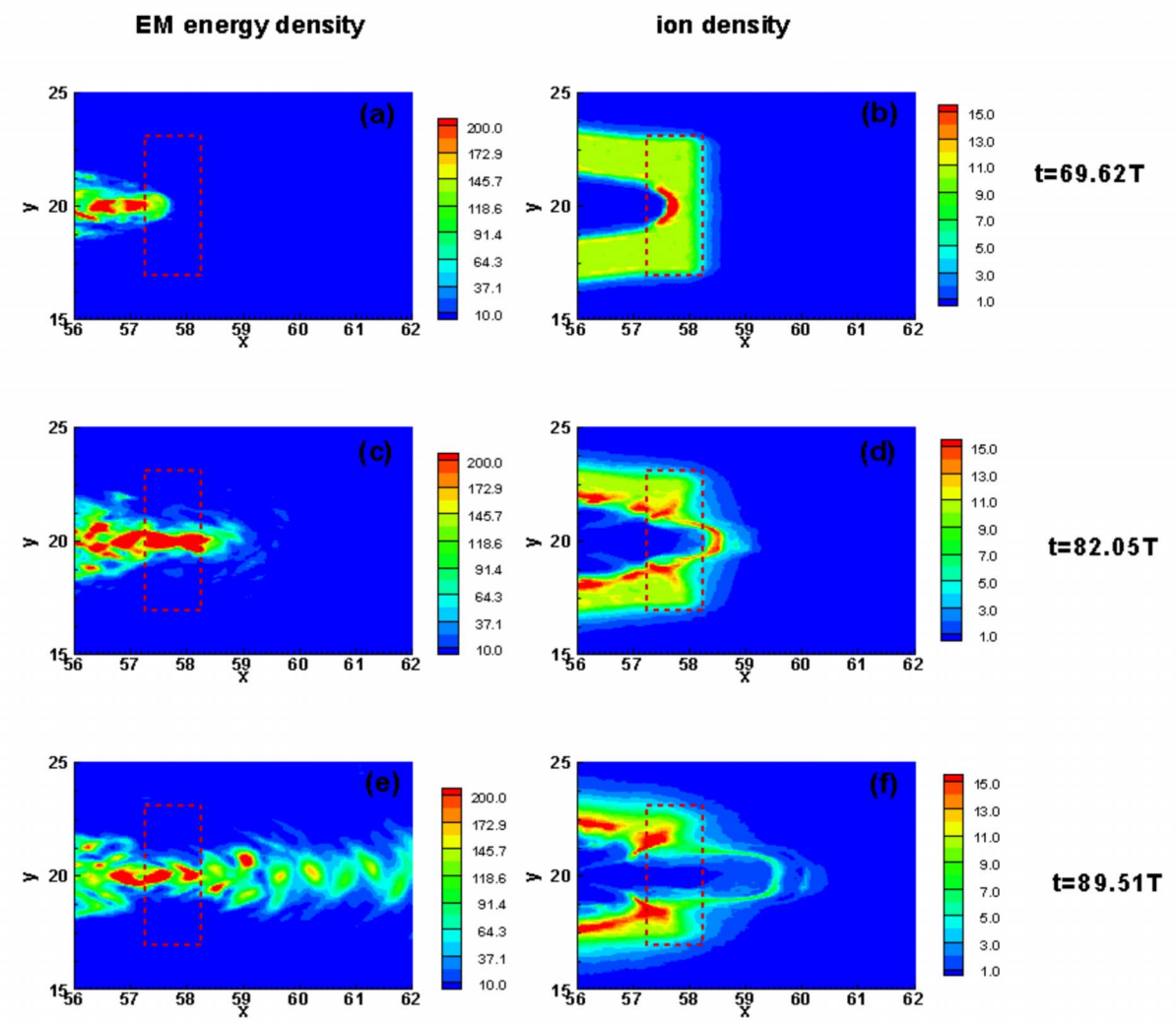

FIG. 5. (Color online) The electromagnetic energy density (left column) and ion density (right column) at $t=69.62T$, $82.05T$, and $89.51T$. The red rectangle marks the initial position of the foil. Note that at $t=89.51T$ the affected part of the target has become very thin (f) and transparent (e).

of MeV) protons in the bunch is correspondingly less than that from existing mechanisms [10,26–28]. The corresponding longitudinal electric field can reach $\sim 3\times 10^{11}$ V/m, which is consistent with the well-known estimate $E \sim k_B T_e / e\lambda_D$ for the target-surface sheath electric field [12], where k_B and λ_D are the Boltzmann's constant and Debye length, respectively.

Figure 7 shows the evolution of the (a) peak ion density and (b) peak ion energy of the leading TNSA ion bunch (red) and the main shock-accelerated ion bunch (black). We see that as expected the ion energy (density) continue to increase (decrease), but at decreasing rate. Since Coulomb repulsion tends to separate the ions by accelerating the faster ones and decelerating the slower ones, the bunches expand as they evolve and the *peak* ion energies increase (even after $t=94T$), but their densities decrease. At $t\sim 94T$ the maximum energy of the shock accelerated ions is above 20 MeV and that for the TNSA ions above 10 MeV. However, very few ions can reach such high energies since at such long times the ion density has become very low.

It is of interest to note that when the foil target is almost punched through by the focused light pulse, the peak ion density is $\sim 5n_c$ for the TNSA bunch and $\sim 10n_c$ for the shock-accelerated bunch. After ten laser periods the peak bunch densities are still above the critical density [Fig. 7(a)] and both bunches are still accelerating after $t=94T$ [Fig. 7(b)]. The effectiveness of the cone-focused light pulse can be attributed to the exceptionally high concentration of light energy along the laser axis within the ~ 1-μm thin pulse.

IV. DISCUSSION

In this paper we have shown that a hollow-cone channel of similar size as the pulse can efficiently nonlinearly focus a laser pulse to a tiny spot (~ 1 μm) of high-intensity light. The action can be attributed to the self-consistent modulational interaction of the outer part of the light pulse with the electrons just inside the cone surface. When the resulting light pulse impinges on a perpendicularly placed plane foil target, the center part of the foil plasma is first compressed

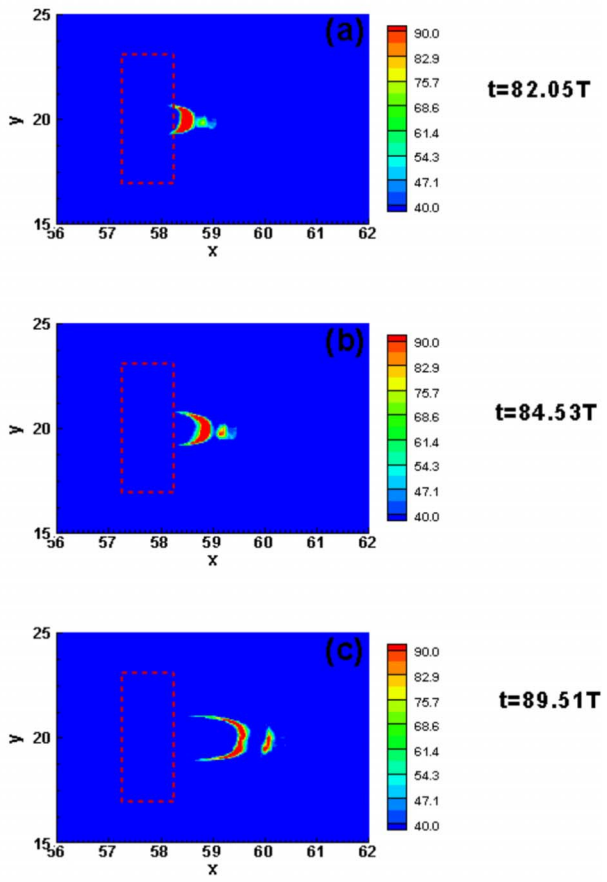

FIG. 6. (Color online) The ion energy density distribution at $t=69.62T$, $82.05T$, and $89.51T$. For clarity, the low-energy density regions have been omitted. Note the spatially highly localized nature of the distribution. The red rectangle marks the initial position of the foil.

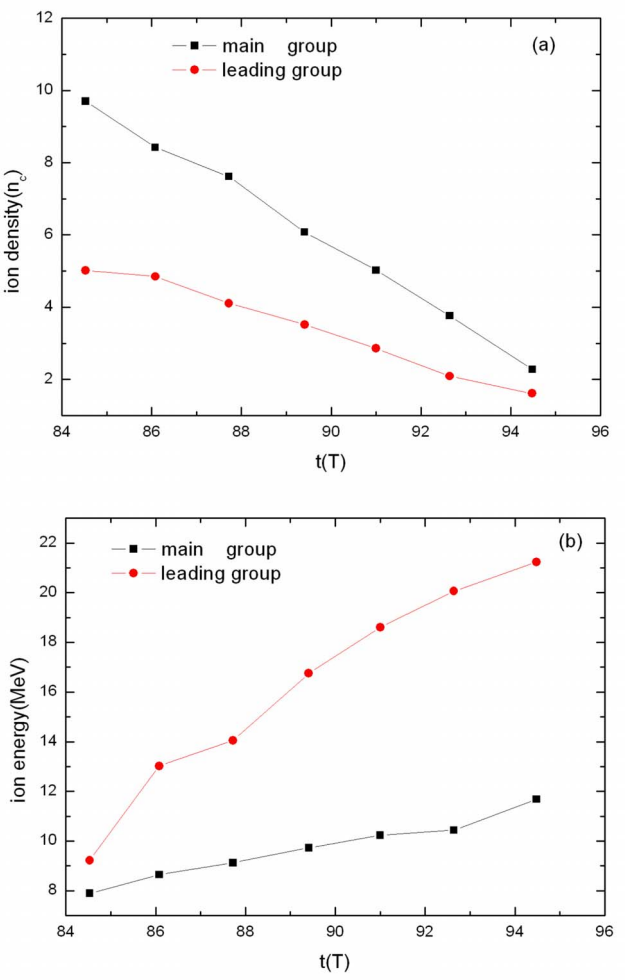

FIG. 7. (Color online) The evolutions of the peak ion density (a) and energy (b) of the leading TNSA (red) and main shock-accelerated (black) ion bunches.

and then indented and pushed out at the target backside. TNSA as well as shock acceleration of all the target ions within the pulse-spot cross section occurs, so that a pair of small-size (1-μm cross section), high-density ($\sim 10n_c$), and high-energy (~ 10 MeV) ion bunches are generated. As the bunches further propagate, their density decrease rapidly, but the maximum ion energy is further increased until Coulomb repulsion becomes ineffective.

The ion acceleration scenario here resembles that of the recently proposed laser-piston acceleration [15] in that a target region of the size of laser spot is completely punched out. The second, or flat-foil, target considered here is of similar thickness, but lower density as that in Ref. [15], and the peak intensity of the input laser here is 4 orders lower. In fact, even after the cone focusing, the peak intensity is still 3 orders of magnitude lower than that required for the laser piston action. It should also be pointed out that the latter requires a very-high-intensity $a=100$ laser pulse with a very sharp leading front, so that the foil is completely transparent at the very beginning of the interaction. In our scheme the tiny cone-focused light pulse has a less abrupt rising front and is much less intense, and the foil is not transparent until the light pulse has almost punched through it. Finally, it may also be of interest to point out that the maximum ion energy obtained here is of similar magnitude as that observed in the LULI experiments under very different laser and target conditions [10].

Our results show that with nonlinear cone focusing it should be possible to realize pistonlike ion acceleration using available lasers. The tip of the cone channel is of a dimension (here 2 μm) comparable to that of the laser pulse and may be difficult to make at present. However, with the rapid advances in nanofabrication technology such a small conical channel should be realizable [31]. Our results on the nonlinear interaction between the laser and the cone wall and the generation of very small laser pulses and ion bunches should be useful in many applications, such as surgery and diagnostics in the micrometer regime. They also suggest that using appropriately designed plasma cavities similar in size to the laser pulse can be a simple and effective method for producing novel light-pulse profiles.

ACKNOWLEDGMENTS

This work was supported by the National High-Tech ICF Committee of China, the National Science Foundation of China (Projects No. 10675024, No. 10734130, No. 10576007, and No. 10576035), National Basic Research Program of China (973 Program) (Grant No. 2007CB815101 and No. 2006CB806004), and Japan-Korea-China Cooperative Project on High Energy Density Sciences for Laser Fusion Energy.

[1] M. D. Perry and G. Mourou, Science **264**, 917 (1994).
[2] P. Gibbon, *Short Pulse Laser Interactions with Matter* (Imperial College Press, London, 2005).
[3] G. A. Mourou, T. Tajima, and S. V. Bulanov, Rev. Mod. Phys. **78**, 309 (2006).
[4] M. Tabak, J. Hammer, M. E. Glinsky *et al.*, Phys. Plasmas **1**, 1626 (1994).
[5] R. A. Snavely, M. H. Key, S. P. Hatchett *et al.*, Phys. Rev. Lett. **85**, 2945 (2000).
[6] E. L. Clark, K. Krushelnick, M. Zepf, F. N. Beg, M. Tatarakis, A. Machacek, M. I. K. Santala, I. Watts, P. A. Norreys, and A. E. Dangor, Phys. Rev. Lett. **85**, 1654 (2000).
[7] A. Maksimchuk, S. Gu, K. Flippo, D. Umstadter, and V. Y. Bychenkov, Phys. Rev. Lett. **84**, 4108 (2000).
[8] E. d'Humières, E. Lefebvre, L. Gremillet, and V. Malka, Phys. Plasmas **12**, 062704 (2005).
[9] M. Borghesi, J. Fuchs, S. V. Bulanov *et al.*, Fusion Sci. Technol. **49**, 412 (2006).
[10] J. Fuchs, P. Antici, E. D'Humière *et al.*, Nat. Phys. **2**, 48 (2006).
[11] S. V. Bulanov, T. Zh. Esirkepov, V. S. Khoroshkov *et al.*, Phys. Lett. A **299**, 240 (2002).
[12] S. C. Wilks, A. B. Langdon, T. E. Cowan *et al.*, Phys. Plasmas **8**, 542 (2001).
[13] J. Denavit, Phys. Rev. Lett. **69**, 3052 (1992).
[14] L. O. Silva, M. Marti, J. R. Davies, R. A. Fonseca, C. Ren, F. Tsung, and W. B. Mori, Phys. Rev. Lett. **92**, 015002 (2004).
[15] T. Esirkepov, M. Borghesi, S. V. Bulanov, G. Mourou, and T. Tajima, Phys. Rev. Lett. **92**, 175003 (2004).
[16] T. Esirkepov, M. Yamagiwa, and T. Tajima, Phys. Rev. Lett. **96**, 105001 (2006).
[17] W. Yu, H. Xu, F. He, M. Y. Yu, S. Ishiguro, J. Zhang, and A. Y. Wong, Phys. Rev. E **72**, 046401 (2005).
[18] S. Fritzler, V. Malka, G. Grillon *et al.*, Appl. Phys. Lett. **83**, 3039 (2003).
[19] T. E. Cowan, J. Fuchs, H. Ruhl *et al.*, Phys. Rev. Lett. **92**, 204801 (2004).
[20] R. Kodama, P. A. Norreys, K. Mima *et al.*, Nature (London) **412**, 798 (2001).
[21] Z. L. Chen, R. Kodama, M. Nakatsutsumi, H. Nakamura, M. Tampo, K. A. Tanaka, Y. Toyama, and T. Tsutsumi, Phys. Rev. E **71**, 036403 (2005).
[22] Y. Sentoku, K. Mima, H. Ruhl *et al.*, Phys. Plasmas **11**, 3083 (2004).
[23] T. Nakamura, H. Sakagami, T. Hohzaki *et al.*, Phys. Plasmas **14**, 103105 (2007).
[24] H. Xu, W. W. Chang, H. B. Zhuo *et al.*, Chin. J. Comput. Phys. **19**, 305 (2002). (in Chinese).
[25] E. L. Lindmann, J. Comput. Phys. **47**, 229 (1982).
[26] A. J. Mackinnon, Y. Sentoku, P. K. Patel, D. W. Price, S. Hatchett, M. H. Key, C. Andersen, R. Snavely, and R. R. Freeman, Phys. Rev. Lett. **88**, 215006 (2002).
[27] M. Hegelich, S. Karsch, G. Pretzler *et al.*, Phys. Rev. Lett. **89**, 085002 (2002).
[28] M. Allen, P. K. Patel, A. Mackinnon, D. Price, S. Wilks, and E. Morse, Phys. Rev. Lett. **93**, 265004 (2004).
[29] E. Lefebvre and G. Bonnaud, Phys. Rev. E **55**, 1011 (1997).
[30] D. W. Forslund and J. P. Freidberg, Phys. Rev. Lett. **27**, 1189 (1971).
[31] K. Ostrikov, Rev. Mod. Phys. **77**, 489 (2005).